

## Infrared and transport properties of $\text{LuFe}_2\text{O}_4$ under electric fields

F. M. Vitucci,<sup>1</sup> A. Nucara,<sup>1</sup> C. Mirri,<sup>1</sup> D. Nicoletti,<sup>1</sup> M. Ortolani,<sup>2</sup> U. Schade,<sup>3</sup> and P. Calvani<sup>1</sup>

<sup>1</sup>*CNR-SPIN and Dipartimento di Fisica, Università di Roma "La Sapienza," Rome, Italy*

<sup>2</sup>*CNR-IFN, Via del Cineto Romano, Roma, Italy*

<sup>3</sup>*Berliner Elektronenspeicherring-Gesellschaft für Synchrotronstrahlung m.b.H., Albert-Einstein Strasse 15, D-12489 Berlin, Germany*

(Received 12 July 2011; published 21 October 2011)

Multiferroic  $\text{LuFe}_2\text{O}_4$  (LFO) exhibits three-dimensional (3D) charge order below  $T_{\text{CO}} \sim 350$  K and strong electroresistance (ER) above a static threshold field  $E_{\text{th}}$ . By measuring simultaneously, in LFO single crystals, the dc current and the far-infrared reflectivity along different axes, we do not detect any insulator-to-metal transition above  $E_{\text{th}}$ . Combined current-temperature measurements confirm that the ER is due to self-heating of LFO, as recently reported. The data can be fit by the standard activation law for an intrinsic semiconductor, with a gap value  $\Delta = 0.57$  eV. This value is consistent with that of the optical gap reported for LFO in the literature.

DOI: [10.1103/PhysRevB.84.153105](https://doi.org/10.1103/PhysRevB.84.153105)

PACS number(s): 78.30.Hv, 75.25.Dk, 63.20.—e

The nontrivial relations between magnetic and electric order in multiferroics<sup>1</sup> have attracted for a long time the attention of both experimentalists and theorists. In magnetoelectric compounds<sup>2,3</sup> the origin of multiferroicity is often attributed to charge-order (CO) phenomena. This is the case for  $\text{LuFe}_2\text{O}_4$ , which exhibits at room temperature both a strong magnetoelectric effect<sup>4,5</sup> and a three-dimensional (3D) CO. Indeed, the transition temperature  $T_{\text{CO}}$  is unusually high, as it ranges (according to different authors) from 320 to 350 K.<sup>6–8</sup> The results that will be presented here are consistent with  $T_{\text{CO}} \simeq 350$  K. Above the transition, the CO is two dimensional (2D).<sup>6</sup>

Under  $T_{\text{CO}}$ , in  $\text{LuFe}_2\text{O}_4$  the electric dipole moments of adjacent iron planes order in opposite directions,<sup>9</sup> while a macroscopic dipole moment is developed when the material is cooled under a moderate external electric field  $\vec{E}$ .<sup>7</sup> This double behavior was explained theoretically in terms of a ferroelectric state very close in energy to the antiferroelectric ground state.<sup>9</sup> Finally, in LFO a marked electroresistance (ER) was observed above a threshold field  $E_{\text{th}}$ ,<sup>4,10</sup> which suggested an insulator-to-metal transition (IMT) at  $E_{\text{th}}$ ,<sup>4</sup> possibly triggered by the CO collapse.<sup>5</sup> However, based on further experiments, the sudden drop in the sample resistivity  $\rho$  at  $E_{\text{th}}$  has been attributed to sample self heating.<sup>11,12</sup> This can result, through a positive feedback, in an avalanche carrier production in the semiconducting material.

The present work first combines infrared spectroscopy and dc transport measurements to provide further experimental basis to the above debate. By measuring the far-infrared reflectivity of LFO single crystals as a function of field and temperature, we explore the possibility of an insulator-to-metal transition in the bulk material causing a field-induced collapse of the 3D ordered phase. To evaluate quantitatively the role of self heating on the dc conductivity, we determine by direct current-temperature measurements the increase in the number of carriers, and we find that it follows the standard law for an intrinsic semiconductor. The resulting gap value  $\Delta$  agrees within 30% with that determined optically.<sup>13</sup>

The reflectivity  $R(\omega)$  of the LFO single crystals was measured under different electric fields  $\vec{E}$  and different polarizations of the radiation field  $\vec{E}_{\text{rad}}$ . In the far infrared,

an IMT would be unambiguously detected through either the appearance of a Drude component and/or a marked shielding of the phonon lines. Moreover, in polar compounds like the oxides, the far-infrared conductivity can detect a massive ionization of self-trapped charges through changes in the polaronic bands in the mid infrared and/or of the infrared active vibration (IRAV) lines in the far infrared.<sup>14,15</sup> Concerning the eventual collapse of CO, it can be monitored through the disappearance of characteristic phonon splittings.<sup>16,17</sup> Therefore we have measured simultaneously the dc transport properties and the crystal temperature, starting from temperatures  $T_0$  between 270 and 400 K, to elucidate the role of current-induced heating. We have thus found that the conventional law for the activation of electrons and holes across the gap in an intrinsic semiconductor fits well to the dc conductivity data. We have also determined the activation energy  $\Delta$  to be  $0.57 \pm 0.04$  eV both below and above  $T_{\text{CO}}$ . This value is close to the optical gap  $\Delta_{\text{opt}}$  reported in the literature.<sup>13</sup>

The experiments were performed on two large single crystals of LFO, grown by the optical floating zone melting method in a flowing argon atmosphere and characterized by x-ray diffraction and Laue imaging at room temperature.<sup>18</sup> In sample 1, hereafter S1 ( $11 \times 4 \times 3$  mm<sup>3</sup>) the largest surface is parallel to the  $ab$  plane, while in S2 ( $8 \times 3 \times 2$  mm<sup>3</sup>) it is  $ac$  oriented. Aluminum/chromium electrical contacts 120 nm thick were deposited by sputtering on a shadow mask. Thin wires were glued on them by silver paint. The current-voltage characteristics and the resistance have been measured by four-probe configurations along both the  $a$  and  $c$  axis, with the setup shown in the inset of Fig. 1. In order to protect the samples and the contacts, the current intensity  $I$  was limited to 100 mA. The sample was thermoregulated at an equilibrium temperature  $T_0$  (at  $E = 0$ ) that was measured by a thermocouple close to the sample. A platinum resistor was also glued onto the sample surface, to measure the surface temperature of the sample  $T_s$  as a function of both field and current.  $T_s$  is the best possible estimate of the bulk temperature, even if a  $T$  gradient will be always present due to the insulating nature of the material. However, we found that, while the thermocouple registered small deviations from  $T_0$ ,  $T_s$  increased up to 40 K during the growth of the current  $I$  to its maximum allowed value.

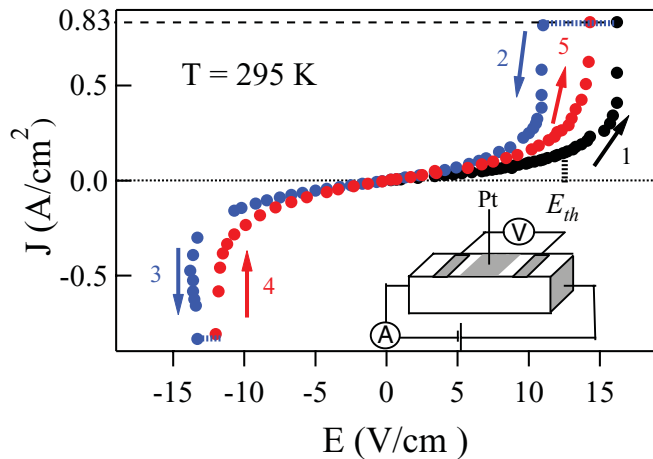


FIG. 1. (Color online) Current density at 295 K for S1, vs a static electric field  $\vec{E}$  parallel to the  $\vec{a}$  axis, that was varied with different procedures (see text). The dashed line marks the limit imposed to the current at 100 mA. The scheme of the experimental set-up for the current-voltage measurements is also shown, with the platinum thermometer Pt glued on the sample surface and obvious significance of the other symbols. During the reflectivity measurements the setup was the same, with the thermometer removed.

A test cycle on sample S1, with the static electric field  $\vec{E}$  parallel to the  $a$  axis, is shown in Fig. 1. The current density  $J$  was measured for  $T_0 = 295$  K, by varying  $\vec{E}$  with different procedures. Branch 1 is obtained by increasing  $E$  monotonically. The current increases approximately linearly, according to an ohmic regime, up to a threshold field  $E_{th} = 12.5$  V/cm. Then  $J$  increases with the applied field, as first reported in Ref. 4, up to its maximum allowed value, according to a power law.<sup>10</sup> When the voltage is decreased, the current starts to decrease and a new  $E_{th} \simeq 7$  V/cm is observed (branch 2). For negative voltage (branches 3 and 4),  $E_{th}$  is about the same as in branch 1. In branch 5,  $E_{th}$  is smaller than in branch 1. The hysteretic behavior of the current in Fig. 1 is due to the internal field created by the polarization of the material (see, e.g., Ref. 19), which in turn is switched on by the external field. Both the hysteresis and the low value of  $E_{th}$  are consistent with the observations of Ref. 10. As  $J$  increased,  $T_s$  increased steadily from its starting value  $T_0 = 295$  K and, at the maximum allowed current of 100 mA, attained about 340 K.

The reflectivity  $R(\omega)$  was measured between 50 and 4000  $\text{cm}^{-1}$  with a Michelson interferometer, after removing the platinum and accurately cleaning the sample surface. The reference was the sample itself, after *in situ* gold coating. We used unpolarized radiation on the  $ab$  surface of S1, and radiation polarized either  $\perp c$  or  $\parallel c$  on the  $ac$  surface of S2. The real part  $\sigma(\omega)$  of the optical conductivity was extracted from  $R(\omega)$  by standard Kramers-Kronig transformations and extrapolations, as in Ref. 16.

In order to understand whether the low-resistance state of LFO may correspond to a bulk metallization of the crystal or not, we performed reflectivity measurements on the  $ab$  plane of S1, both at zero field and under  $E > E_{th}$  (i.e. with  $I = 100$  mA), at different starting temperatures  $T_0$ . The results are shown in Fig. 2(a). As one can see, the reflectivity is

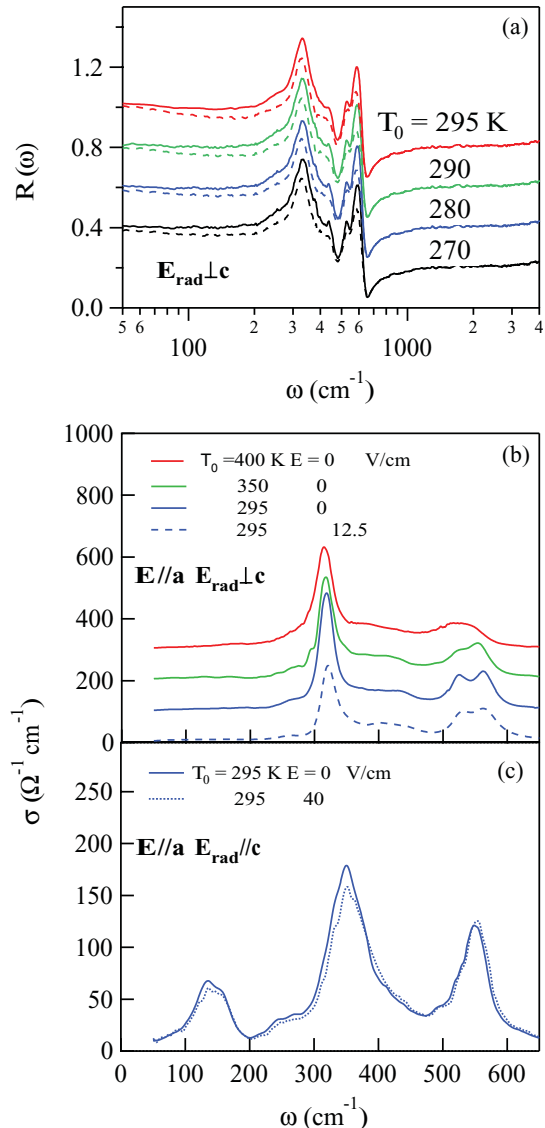


FIG. 2. (Color online) (a) Reflectivity for  $E = 0$  (full lines) and for  $E > E_{th}$  (100 mA flowing through the sample, dashed lines) measured on the  $ab$  plane of the LFO crystal S1 with unpolarized radiation. For sake of clarity, the spectra at different temperatures have been shifted vertically by 0.2. (b) Far-infrared optical conductivity of the  $ab$  plane of S1 at 295 K, for  $E = 0$  and  $E > E_{th}$ , compared with those at zero field at  $T_{CO}$  and above. (c) Optical conductivity of S2 at 295 K for  $E > E_{th}$  and for  $E = 0$ , with  $\vec{E}_{rad}$  polarized along the  $\vec{c}$  axis and  $\vec{E}$  along the  $\vec{a}$  axis.

insensitive to  $E$  (or  $J$ ) at all temperatures, except for a slight broadening of the phonon absorption due to sample heating. None of the phenomena associated with a possible IMT in the crystal bulk above  $E_{th}$  is observed in Fig. 2(a). Not only does the far-infrared reflectivity decrease instead of increasing, confirming a growth in  $T_s$ , but the phonon modes are not appreciably shielded and there is no Drude contribution down to the lowest measured frequency.

Figure 2(b) shows the optical conductivity extracted from the reflectivity of S1 at 295 K, at  $E = 0$  and  $E > E_{th}$ , compared with those at higher temperatures and zero field. The doublet around 550  $\text{cm}^{-1}$ , characteristic of the 3D

charge order,<sup>16,17</sup> is clearly present at 295 K and can still be distinguished, in the form of a shoulder of the main peak, at 350 K. At  $T = 400$  K the doublet has disappeared, indicating that the transition from the 3D to the 2D ordered phase is completed. These temperatures could not be measured with the thermometer glued on the sample, but close to it. As one can see, for  $T_0 = 295$  K and  $I = 100$  mA,  $\sigma(\omega)$  is similar to that at zero field, except for a broadening of the phonon lines. This confirms that the sample is still in the 3D ordered phase, even if  $T_s$  is close to  $T_{CO}$ . For sake of completeness, the optical response of LFO was also probed by polarizing  $\vec{E}_{rad}$  along the crystal  $c$  axis while keeping  $\vec{E}$  along the  $a$  axis. These experiments were performed starting from room temperature on crystal S2. The resulting optical conductivity is reported in Fig. 2(c) for  $E = 0$  and  $E = 40$  V/cm, a value corresponding to 100 mA flowing along the  $c$  axis (see next subsection). Once again, no hint of sample metallization is detected in the infrared spectrum.

The results of simultaneous measurements in S1 of  $J$ ,  $E$ , and of the surface temperature  $T_s$  are reported in Fig. 3. Panel (a) plots the zero-frequency conductivity  $\sigma_{dc} = J/E$  versus  $T_s$ , with  $\vec{E}$  parallel to  $\vec{a}$ , for different starting temperatures  $T_0$  below and above the transition temperature  $T_{CO}$ . As one can see, the increase in the conductivity, which mimics that of  $J$  versus  $E$  in Fig. 1, is accompanied by a marked temperature increase  $\Delta T_s$ . If one assumes that LFO is an intrinsic semiconductor and neglects the change in the carrier scattering rate within  $\Delta T_s$ , one has  $\sigma_{dc} \propto (n + p)$ , where  $n$  ( $p$ ) is the electron (hole) density, given by

$$n = p = AT_s^{3/2} \exp(-\Delta/2k_B T_s). \quad (1)$$

Therein  $A$ , which includes the effective masses of both electrons and holes, is assumed constant along each  $\sigma_{dc}$  curve, for any given  $T_0$ . The fits to Eq. (1) are the solid lines in Fig. 3(a). Small deviations are evident in the initial part of the highest-temperature curves, where the change with  $T_s$  of the scattering rate is not overwhelmed by that of the carrier density. However, all fitting curves, for  $T_0$  both below and above  $T_{CO}$ , provide an energy gap  $\Delta = 0.57 \pm 0.04$  eV. This value is consistent with the edge of the optical gap reported by Xu *et al.*,<sup>13</sup> who measured  $\Delta_{opt} \simeq 0.45$  eV around room temperature. They identified the gap with the edge of a broad infrared contribution which is assigned to indirect, phonon-assisted, interband transitions. Their optical experiment, which detects Frank-Condon adiabatic transitions, showed a smooth decrease<sup>13</sup> in  $\Delta_{opt}$  across  $T_{CO}$ , that the present dc measurements do not detect. The fact that the  $\sigma_{dc}$  values belonging to different curves at the same  $T_s$  in Fig. 3(a) differ from each other can be understood by considering that they correspond to different applied fields  $E$ , and therefore (i) to a different polarization of the sample, and (ii) to different temperature gradients between the bulk and the surface.

Figure 3(b) shows  $J$  versus  $E$  in S2 for  $\vec{E}$  parallel either to the  $\vec{a}$  axis or to the  $\vec{c}$  axis, in both cases with the current limited to 100 mA. The corresponding threshold fields are much different, being  $E_{th} \simeq 12$  V/cm along  $\vec{a}$  (as in S1 within errors) and  $\sim 40$  V/cm along  $\vec{c}$ , somewhat smaller than in Ref. 10.

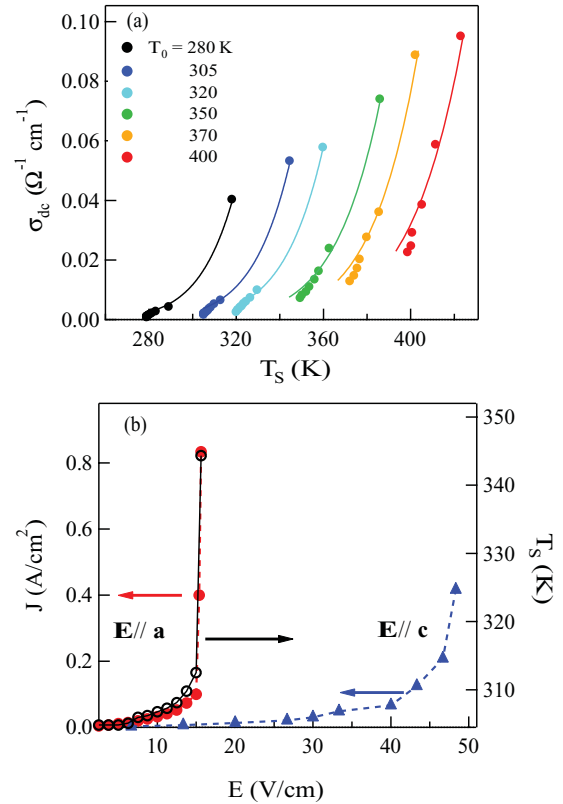


FIG. 3. (Color online) (a) Zero-frequency conductivity in S1 vs sample temperature for different initial temperatures  $T_0$ . The solid lines are fits to Eq. (1); the dashed line is  $\sigma_{dc}(T_0)$ , as measured at  $E \simeq 0$ . (b) Current density (left scale) in S2 for the electric field  $\vec{E}$  applied along  $\vec{a}$  (dots) and  $\vec{c}$  (triangles). The circles are  $T_s$  values (right scale) measured vs the applied  $E$  simultaneously with  $J$ .

The difference reflects the strongly anisotropic structure of this layered compound. The close relation between current increase and heating is also confirmed in Fig. 3(b), where  $J$  versus  $E$  along  $\vec{a}$  (left scale, dots) is compared with the simultaneously measured  $T_s$  (right scale, circles) versus  $E$ . Also, the field threshold value  $E_{th}$  is the same for both.

In conclusion, we have measured both the dc and infrared conductivity of two single crystals of the multiferroic compound  $\text{LuFe}_2\text{O}_4$ , under static electric fields  $\vec{E}$ , in order to better understand the large electroresistance effect reported in the recent literature. It is confirmed that, above a threshold field  $E_{th}$ , whose value shifts from 12.5 V/cm for  $\vec{E} \parallel ab$ , to 40 V/cm for  $\vec{E} \parallel c$ , the current density increases steeply. The  $J$  versus  $E$  plots are symmetric for reversal of  $\vec{E}$  but show a hysteretic behavior due to the ferroelectricity of the material. However, the bulk optical conductivity does not show any indication of an insulator-to-metal transition, nor of a collapse of the 3D charge order induced by the field, at  $E_{th}$  or above. This has been verified with the radiation field both along the  $a$  axis and along the  $c$  axis. Combined current-temperature measurements confirm that the large current increase above  $E_{th}$  is due to a self-heating of the sample. This starts below  $E_{th}$  and is caused, due to the semiconducting nature of the material, by a positive current-heating-current feedback. Indeed, we could fit all the

$\sigma_{dc}$  versus  $T_s$  curves, both below and above the 3D charge ordering temperature  $T_{CO} \simeq 350$  K, by a standard activation law for an intrinsic semiconductor. The value found for the gap  $\Delta = 0.57 \pm 0.04$  eV is consistent with that edge of interband transitions measured optically by other authors. We did not find appreciable changes in  $\Delta$  across the 3D-2D charge-order transition.

We are indebted to Y. Sun who provided the single crystals used in this experiment. We also acknowledge the Helmholtz-Zentrum Berlin-Electron storage ring BESSY II for provision of synchrotron radiation at the IRIS beamline. The research leading to these results has been partially funded by the EU's Seventh Framework Programme (FP7/2007-2013) under Grant No. 226716.

- 
- <sup>1</sup>N. A. Hill, *J. Phys. Chem. B* **104**, 6694 (2000).  
<sup>2</sup>M. Fiebig, *J. Phys. D* **38**, R123 (2005).  
<sup>3</sup>A. Feteira, D. C. Sinclair, I. M. Reaney, Y. Somiya, and M. T. Lanagan, *J. Am. Ceram. Soc.* **87**, 1082 (2004).  
<sup>4</sup>C. Li, X. Zhang, Z. Cheng, and Y. Sun, *Appl. Phys. Lett.* **93**, 152103 (2008).  
<sup>5</sup>F. Wang, C.-H. Li, T. Zou, Y. Liu, and Y. Sun, *J. Phys. Condens. Matter* **22**, 496001 (2010).  
<sup>6</sup>Y. Yamada, K. Kitsuda, S. Nohdo, and N. Ikeda, *Phys. Rev. B* **62**, 12167 (2000).  
<sup>7</sup>N. Ikeda, H. Ohsumi, K. Ohwada, K. Ishii, T. Inami, K. Kakurai, Y. Murakami, K. Yoshii, S. Mori, Y. Horibe, and H. Kito, *Nature (London)* **436**, 1136 (2005).  
<sup>8</sup>A. B. Harris and T. Yildirim, *Phys. Rev. B* **81**, 134417 (2010).  
<sup>9</sup>M. Angst, R. P. Hermann, A. D. Christianson, M. D. Lumsden, C. Lee, M.-H. Whangbo, J.-W. Kim, P. J. Ryan, S. E. Nagler, W. Tian, R. Jin, B. C. Sales, and D. Mandrus, *Phys. Rev. Lett.* **101**, 227601 (2008).  
<sup>10</sup>L. J. Zeng, H. X. Yang, Y. Zhang, H. F. Tian, C. Ma, Y. B. Qin, Y. G. Zhao, and J. Q. Li, *Europhys. Lett.* **84**, 57011 (2008).  
<sup>11</sup>J. Wen, G. Xu, G. Gu, and S. M. Shapiro, *Phys. Rev. B* **81**, 144121 (2010).  
<sup>12</sup>B. Fisher, J. Genossar, L. Patlagan, and G. M. Reisner, *J. Appl. Phys.* **109**, 084111 (2011).  
<sup>13</sup>X. S. Xu, M. Angst, T. V. Brinzari, R. P. Hermann, J. L. Musfeldt, A. D. Christianson, D. Mandrus, B. C. Sales, S. McGill, J.-W. Kim, and Z. Islam, *Phys. Rev. Lett.* **101**, 227602 (2008).  
<sup>14</sup>P. Calvani, *Riv. Nuovo Cimento* **20**, 1 (2001).  
<sup>15</sup>P. Calvani, M. Capizzi, S. Lupi, and G. Balestrino, *Europhys. Lett.* **31**, 473 (1995).  
<sup>16</sup>F. M. Vitucci, A. Nucara, D. Nicoletti, Y. Sun, C. H. Li, J. C. Soret, U. Schade, and P. Calvani, *Phys. Rev. B* **81**, 195121 (2010).  
<sup>17</sup>X. S. Xu, J. de Groot, Q.-C. Sun, B. C. Sales, D. Mandrus, M. Angst, A. P. Litvinchuk, and J. L. Musfeldt, *Phys. Rev. B* **82**, 014304 (2010).  
<sup>18</sup>C. H. Li, F. Wang, Y. Liu, X. Q. Zhang, Z. H. Cheng, and Y. Sun, *Phys. Rev. B* **79**, 172412 (2009).  
<sup>19</sup>D. J. Fu, J. C. Lee, S. W. Choi, S. J. Lee, T. W. Kang, M. S. Jang, H. I. Lee, and Y. D. Woo, *Appl. Phys. Lett.* **81**, 25207 (2002).